

## A NEW NEARBY GALAXY TABLE\*

DAVID M. FRENCH, BART P. WAKKER  
 Department of Astronomy, University of Wisconsin - Madison  
*Draft version March 20, 2018*

### ABSTRACT

We present an all-sky catalog of galaxies in the nearby,  $cz \leq 10,000 \text{ km s}^{-1}$  redshift range. We have sourced published data available through the NASA Extragalactic Database (NED), the NASA/IPAC Infrared Science Archive (IRSA), the Third Reference Catalogue of Bright Galaxies (RC3), and the Tully (2015) 2MASS galaxy group catalog. We have taken steps to homogenize the data by converting diameter measurements to 2MASS values, and employing outlier rejection to choose representative values for position angle, inclination, redshift-independent distance, and  $B$ -band magnitude.

*Subject headings:* IGM, CGM, galaxies

### 1. INTRODUCTION

Galaxy catalogs at once seem somewhat outdated in the age of the internet, yet still frustratingly necessary. The ideal solution of an all-sky and all-object online database containing homogenized information has not been completely realized, even as the NASA Extragalactic Database (NED), VizieR, SIMBAD and others fulfill some of these requirements. Each of these databases offer slightly different sets of information on their objects however, and there is often no straightforward way for extracting all the parameters needed. For example, there is no way to return the diameters of all known galaxies in a particular redshift range. Furthermore, comparing and choosing between disparate measurements of common galaxy parameters (e.g., diameter, inclination, magnitude, distance, etc.) is not trivial when a large sample is required. The need for a simple, highly complete lookup nearby galaxy catalog remains.

This catalog was born from

In an effort to study the circumgalactic medium (CGM) in the nearby universe we have constructed a catalog of galaxies with  $cz \leq 10,000 \text{ km s}^{-1}$ . All of the data included here is publicly available through the NASA Extragalactic Database (NED) and the NASA/IPAC Infrared Science Archive (IRSA). We have endeavored in various ways to create a single, homogeneous catalog.

This catalog is not meant to be entirely robust or comprehensive - rather it's purpose is to present a common batch of parameters for nearby galaxies in a easily retrievable and machine-readable manner. We have nonetheless endeavored to provide reasonable error estimates on all derivations and for as many observed quantities as possible.

We originally began compiling this data base as a tool to aid in the matching of galaxies to absorption detected in background QSO spectra. As effort in it's creation mounted, we decided that it could prove useful to the community.

Some caveats:

1. This is not the result of a targeted survey or observing program, so it's coverage and completeness is inherently non-uniform. We have endeavored to quantify this non-uniformity in Section XXXX.

2. The quality of the data and observational errors are

difficult to determine. We present this dataset as more of a convenient "quick-look" directory than a scientifically rigorous data product.

In Section 2 we discuss our data retrieval methods and handling of distance and velocity measurements. In Section 3, we provide explanation and details for galaxy attribute included in the catalog (i.e., the columns). We discuss caveats and limitations in Section 4. Throughout this catalog we have adopted the cosmology  $H_0 = 71 \text{ km s}^{-1} \text{ Mpc}^{-1}$ ,  $\Omega_m = 0.27$ , and  $\Omega_\Lambda = 0.73$ .

### 2. DATA

#### 2.1. Galaxy Data Retrieval

The goal of this study relies on knowing the locations and properties of all galaxies near detected Ly $\alpha$  absorption lines. To facilitate this, we have constructed a dataset of all  $z \leq 0.033$  ( $cz \leq 10,000 \text{ km s}^{-1}$ ) galaxies with published data available through the NASA Extragalactic Database (NED).

The galaxy dataset contains over 130,000 entries, and includes data from SDSS, 2MASS, 2dF, 6dF, RC3, and many other, smaller surveys. Our criteria for including a galaxy in this dataset is only a published redshift which places the galaxy in the  $cz \leq 10,000 \text{ km s}^{-1}$  velocity range. This restriction leads to a completeness limit of  $B \lesssim 18.7 \text{ mag}$ , or  $\sim 0.2L_*$ , at  $cz = 10,000 \text{ km s}^{-1}$ , and progressively better towards lower velocities (see Figure 1). This limit will vary depending on which major surveys include a particular region of the sky. The major contributor is whether or not SDSS data is available, which begins around  $cz = 5,000 \text{ km s}^{-1}$ . Figure 1 is split into 4 velocity bins to illustrate this. Our data is complete down to  $\sim 0.1L_*$  in the first bin,  $0 \leq cz \leq 2,500 \text{ km s}^{-1}$ . At slightly higher velocity,  $2500 \leq cz \leq 6000 \text{ km s}^{-1}$ , the completeness falls to barely better than  $\sim 1.0L_*$  as we move past the near and well studied galaxies, but have yet to reach the footprint of deep all sky surveys. SDSS data becomes available in the last two bins, spanning  $6000 \leq cz \leq 10,000 \text{ km s}^{-1}$ , and correspondingly completeness remains high down to the SDSS limits of  $B \lesssim 18.7 \text{ mag}$ , or  $\sim 0.2L_*$  at  $cz = 10,000 \text{ km s}^{-1}$ .

#### 2.2. Distances & Velocities

For XXXX% of galaxies, a redshift-independent distance estimate is available. In this case  $d_{best}$  is set to

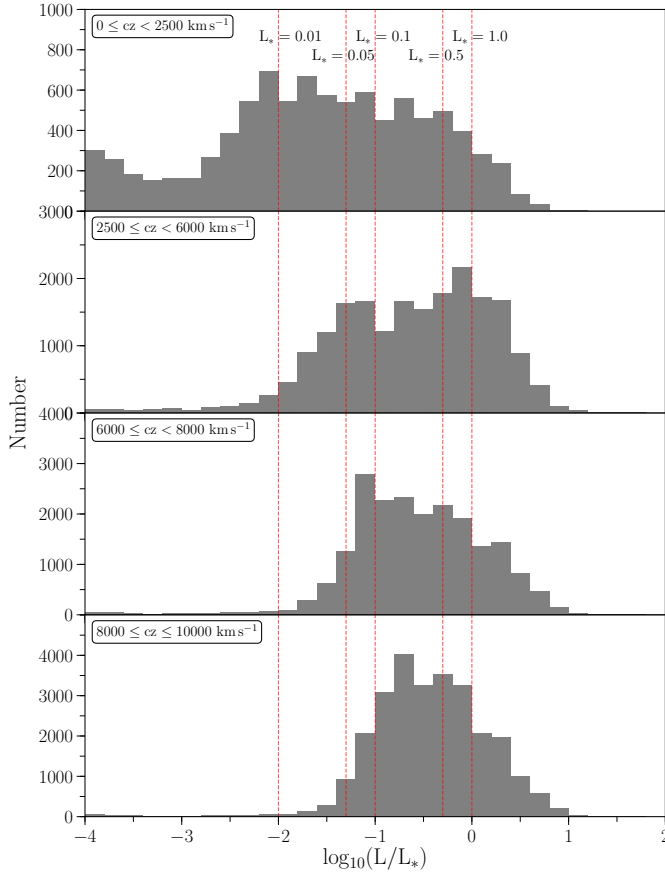


**Figure 1.** Distribution of  $L/L_*$  values for all galaxies in the dataset. Black vertical lines highlight 1, 0.5, 0.1, 0.05 and 0.01  $L_*$ . The turnoff in the distribution for each region reveals the corresponding completeness. We are complete to almost  $0.01L_*$  out to  $2500 \text{ km s}^{-1}$ ,  $0.5L_*$  between  $2500 \leq cz \leq 5000 \text{ km s}^{-1}$ ,  $0.1L_*$  between  $6000 \leq cz \leq 8000 \text{ km s}^{-1}$ , and  $0.3L_*$   $8000 \leq cz \leq 10000 \text{ km s}^{-1}$ .

the mean of all available redshift-independent distance estimates, and  $d_{err_{best}}$  is set to the standard deviation on the mean. When only a redshift is available, we set  $d_{best}$  equal to the Hubble law distance as calculated with  $H_0 = 71 \text{ km s}^{-1} \text{ Mpc}^{-1}$ , and  $d_{err_{best}}$  equal to 10% of the resulting distance estimate. Nearby, the uncertainty is dominated by deviations from the Hubble Flow due to, e.g., the Local Group, and at larger distances the uncertainty in  $H_0$  becomes dominant. The distance error for any particular galaxy is difficult to ascertain, but at 10% error should contain the true  $1 - \sigma$  error across our full redshift range.

All galaxies with zero or negative  $v_{hel}$  have  $d_{best}$  set to 1 Mpc, and  $d_{err_{best}}$  to 0.5 Mpc.

### 3. THE CATALOG

The following section describes the contents of each column in the order it appears in the catalog. Null values are marked in one of three ways. Columns containing strings have the null value of 'x', those containing integers have null value '-99', and those containing floating point entries have null value '-99.99'.

#### 3.1. Name

Our preferred name for the galaxy. The ordering is as follows: NGC, IC, MRK, UGC, UGCA, PHL, 3C, SBS, MCG, ESO, TON, TONS, PGC, PG, PB, FGC, HS, HE, KUG, IRAS, RX, CGCG, KAZ, FCC, FAIRALL, HOLM, IZw, IIZw, IIIZw, IVZw, VZw, VIZw, VIIZw, VIIIZw, IRAS, IRASF, KISS, KISSR, FBQS, LBQS, PKS, SDSS, VCC, 2MASS, 2DF, 6DF, HIPASS, 2MASX.

If none of these are available, we adopt the NED preferred name.

#### 3.2. NEDname

The preferred name for the galaxy in the NED database.

#### 3.3. z

The NED redshift for the galaxy.

#### 3.4. RAdeg

Equatorial right ascension coordinate in degrees (J2000.0 epoch).

#### 3.5. DEdeg

Equatorial declination coordinate in degrees (J2000.0 epoch).

#### 3.6. RAh

Equatorial right ascension hour coordinate (J2000.0 epoch).

#### 3.7. RAm

Equatorial right ascension minute coordinate (J2000.0 epoch).

#### 3.8. RAs

Equatorial right ascension second coordinate (J2000.0 epoch).

#### 3.9. DE-

Equatorial declination coordinate sign (J2000.0 epoch).

#### 3.10. DEd

Equatorial declination degree coordinate (J2000.0 epoch).

#### 3.11. DEm

Equatorial declination minute coordinate (J2000.0 epoch).

#### 3.12. DES

Equatorial declination second coordinate (J2000.0 epoch).

#### 3.13. GLON

Galactic longitude coordinate.

#### 3.14. GLAT

Galactic latitude coordinate.

### 3.15. *Vhel*

Heliocentric radial velocity in  $\text{km s}^{-1}$  units. As done by NED, we do not make any relativistic correction to these velocities.

### 3.16. *vcorr*

Virgocentric flow-corrected velocity. Following Geller & Huchra (1982), this corresponds to a  $300 \text{ km s}^{-1}$  velocity toward  $R.A. = 186^\circ.7833$ ,  $decl. = 12^\circ.9333$ .

### 3.17. *distvcorr*

Distance calculated from *vcorr* with a Hubble constant of  $H_0 = 71 \text{ km s}^{-1} \text{ Mpc}^{-1}$ .

### 3.18. *RID\_mean*

Mean redshift independent distance from the NED-D catalog (Tully et al. 2009). This is the arithmetic mean of the available measurements and therefore does not correspond to any single measurement in particular.

### 3.19. *RID\_median*

Median redshift independent distance from the NED-D catalog. This is not the arithmetic median of the set, but rather the published distance value *closest* to the median. The method used for this distance estimate is given by *distIndicator* (Section 3.50).

### 3.20. *RID\_std*

Standard deviation of all redshift independent distance measurements.

### 3.21. *RID\_min*

Minimum published redshift independent distance.

### 3.22. *RID\_max*

Maximum published redshift independent distance.

### 3.23. *bestDist*

Our chosen best distance estimate. *dist\_best* is equal to *RID\_median* when a redshift independent distance is available, and otherwise defaults to *distvcorr*.

### 3.24. *e\_bestDist*

The error on *bestDist*. *e\_bestDist* is equal to *RID\_std* when a redshift independent distance is available. Otherwise, *e\_bestDist* is set to 10% of *distvcorr* when *vcorr*  $\geq 0$ , and 50% of *distvcorr* if *vcorr*  $< 0$ .

### 3.25. *MajDiam\_ang*

Major axis diameter in units of arcsec.

We have homogenized the galaxy data beyond the steps taken by NED by normalizing diameter measurements to 2MASS  $K_s$ -band values. Most galaxies in NED have measures of inclination, position angle and diameter available in several different bands, so in order to make more meaningful comparisons we choose one band for all measurements. We chose 2MASS values for this because it was an all-sky survey, and represents the largest fraction of available galaxy data. Physical galaxy diameters are derived from 2MASS  $K_s$  “total” angular diameter measurements and galaxy distances. 2MASS  $K_s$  “total”

diameter estimates are surface brightness extrapolation measurements and were derived by the 2MASS team as

$$r_{tot} = r' + a(\ln(148))^b, \quad (1)$$

where  $r_{tot}$  is defined as the point where the surface brightness extends to 5 disk scale lengths,  $r'$  is the starting point radius ( $> 5'' - 10''$  beyond the nucleus, or core influence), and  $a$  and  $b$  are Sersic exponential function scale length parameters ( $f = f_0 \exp(-r/a)^{(1/b)}$ , see Jarret et al. 2003 for a full description). Approximately 50% of all the galaxies have this 2MASS  $K_s$  “total” diameter. Of the remainder, 20% have SDSS diameters, 3% have diameters from other surveys, and 27% have no published diameter.

For galaxies with multiple published measurements from different facilities, we have derived linear fits in order to convert between them. The orthogonal distance regression (ODR) algorithm as implemented by the Fortran code ODRPACK (and the Python wrapped version included in the Scipy package) was used to derive these best fits and their associated errors. ODR, compared to the more common linear regression algorithm, assumes errors in both x- and y-coordinates and thus minimizes the orthogonal distance between both dependent and independent data and the fit. We then ranked the available surveys in order of goodness of fit to 2MASS values. The fits for each survey are listed in Table 1.

A significant fraction of galaxies have irregular, incomplete, or otherwise suspect diameter data as published in NED. For example, some have 2MASS  $K_s$  “total” diameters available, but the published axis ratio is either greater than 1, or otherwise significantly deviates from that found in other surveys. Furthermore, often our highest ranking diameter survey has incomplete data (such as a missing axis ratio or position angle measurement). For our purposes we want to choose a single, representative value for each parameter. We decision tree is as follows: 1) we choose the highest ranking measurement available, and choose the largest major-axis diameter value when multiple are available from the same facility, 2) we choose the highest ranking axes ratio, preferentially selecting the value from the measurement chosen in (1), but rejecting a ratio = 1 when the average ratio of all measurements is less than 1, 3) we choose the highest ranking position angle measurement, again preferentially selecting the value included in (1).

Finally, we check to see if our initial choices are outliers using a version of the Iglewicz-Hoaglin Method, a median absolute deviation algorithm (Iglewicz & Hoaglin 1993). Through trial-and-error we set our outlier thresholds at 14.0 for major axis diameters, 3.5 for position angles, and 2.5 for axis ratios. Smaller threshold values indicate a stricter outlier rejection. If our initial choice of any of these values is flagged as an outlier, we choose the next highest-ranking, non-outlier value. The decision of diameter, ratio and position angle for each galaxy is included in the 3.38, 3.39, and 3.40 columns.

### 3.26. *MinDiam\_ang*

Minor axis diameter in units of arcsec. See 3.25 for a complete discussion.

### 3.27. *e\_MajDiam\_ang*

Survey Name	m	y-intercept	Fraction of Total
K <sub>s</sub> (2MASS isophotal)	$1.765 \pm 0.003$	$1.31 \pm 0.06$	XXX
POSS1 103a-O	$0.869 \pm 0.007$	$17.6 \pm 0.4$	XXX
POSS1 103a-E	$1.055 \pm 0.043$	$26.22 \pm 1.98$	XXX
ESO-LV "Quick Blue" IIa-O	$0.81 \pm 0.02$	$-9.7 \pm 1.4$	XXX
r (SDSS Isophotal)	$1.033 \pm 0.005$	$0.84 \pm 0.17$	XXX
RC3 D_0 (blue)	$1.040 \pm 0.009$	$1.29 \pm 0.58$	XXX
RC3 D_25, R_25 (blue)	$1.107 \pm 0.009$	$3.09 \pm 0.60$	XXX
r (SDSS Petrosian)	$4.728 \pm 0.032$	$3.38 \pm 0.21$	XXX
r (SDSS deVaucouleurs)	$3.49 \pm 0.04$	$14.45 \pm 0.21$	XXX
r (SDSS de Vaucouleurs)	$2.70 \pm 0.04$	$15.64 \pm 0.22$	XXX
RC3 A_e (Johnson B)	$2.25 \pm 0.06$	$19.2 \pm 1.8$	XXX
r (SDSS Exponential)	$8.24 \pm 0.06$	$7.7 \pm 0.2$	XXX
B (Johnson)	$1.24 \pm 0.09$	$-25.3 \pm 9.7$	XXX
R (Kron-Cousins)	$1.47 \pm 0.14$	$-35.9 \pm 14.4$	XXX
ESO-Uppsala "Quick Blue" IIa-O	$1.06 \pm 0.02$	$-13.4 \pm 1.4$	XXX
ESO-LV IIIa-F	$4.65 \pm 0.13$	$23.02 \pm 0.92$	XXX

**Table 1**  
Diameter fits in order of quality.

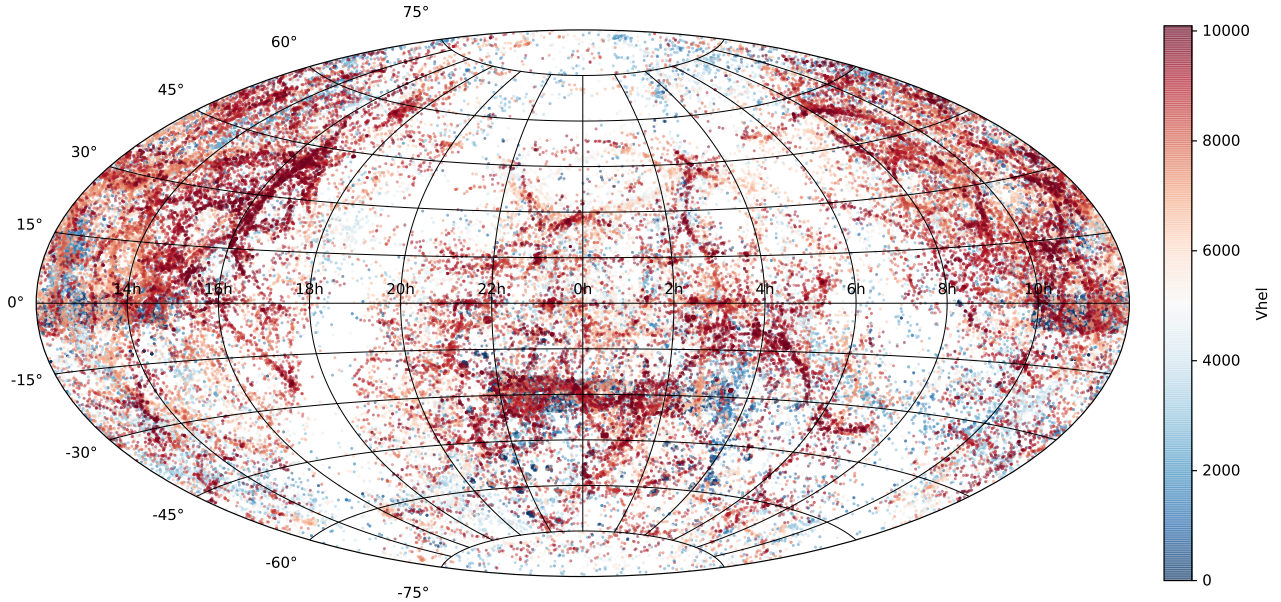


**Figure 2.** Position of all galaxies on plotted in Aitoff projection and colored according to heliocentric velocity.

Major axis diameter error. This error is purely a result of the fit to K<sub>s</sub> (2MASS) values, and thus does not take into account any observational errors.

### 3.28. $e\_MinDiam_{ang}$

Minor axis diameter error. This error is purely a result of the fit to K<sub>s</sub> (2MASS) values, and thus does not take into account any observational errors.

### 3.29. $MajDiam$

Linear major axis diameter in units of kpc, calculated using *bestDist*. See 3.25 for a complete discussion.

### 3.30. $MinDiam$

Linear minor axis diameter in units of kpc, calculated using *bestDist*. See 3.25 for a complete discussion.

### 3.31. $e\_MajDiam$

Linear major axis diameter error. This error is purely a result of the fit to K<sub>s</sub> (2MASS) values, and thus does not take into account any observational errors.

### 3.32. $e\_MinDiam$

Linear minor axis diameter error. This error is purely a result of the fit to K<sub>s</sub> (2MASS) values, and thus does not take into account any observational errors.

### 3.33. $R_{vir}$

Virial radius estimate calculated as

$$\log R_{vir} = 0.69 \log D + 1.24. \quad (2)$$

This follows the parametrization of Stocke et al. (2013) relating a galaxy's luminosity to its virial radius, com-

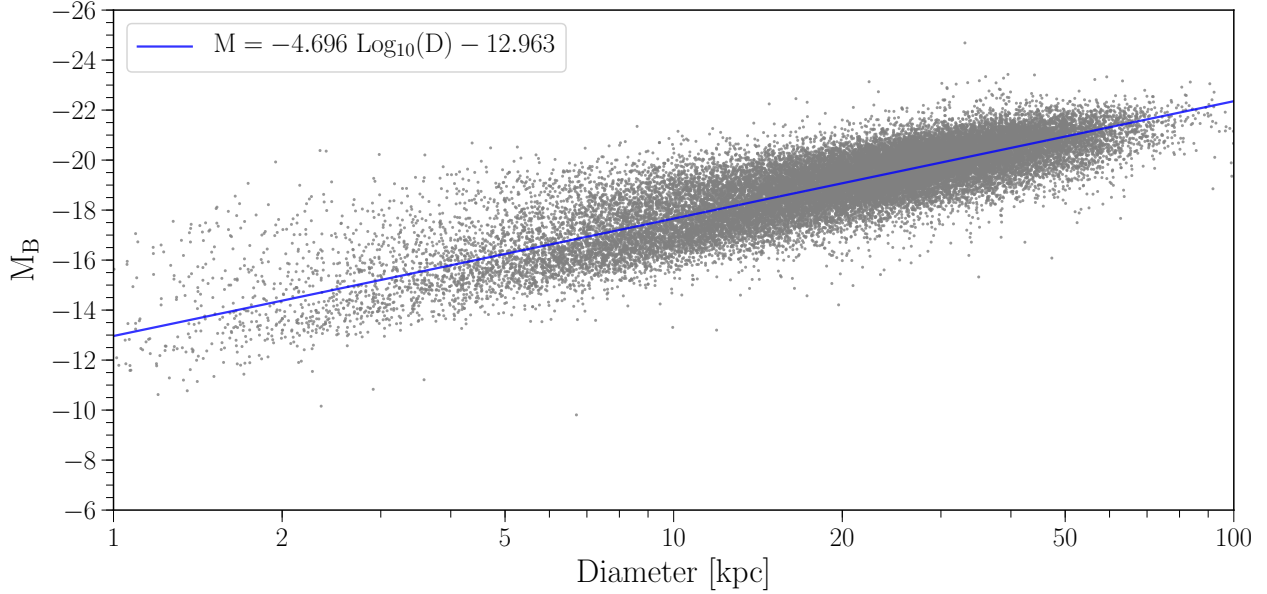


**Figure 3.** Relationship between absolute  $B$ -band magnitude and physical diameter for all galaxies with available data. Data are in grey, and a least-squares fit is shown in blue. The function form of this fit is  $M = a \log_{10}(D) + b$ , with fit parameters  $a = -4.696 \pm 0.01$  and  $b = -12.963 \pm 0.01$ .

binned with the Wakker & Savage (2009) empirical relation between diameter and luminosity (see Wakker et al. 2015 and references therein for further details).

#### 3.34. *inc*

Galaxy inclination calculated as *inc.* =  $\cos^{-1}(\text{minor}/\text{major})$  in units of degrees.

#### 3.35. *adjustedInc*

Galaxy inclination calculated assuming a finite disk thickness following Heidmann et al. (1972a):

$$\cos(i) = \sqrt{\frac{q^2 - q_0^2}{1 - q_0^2}}, \quad (3)$$

where  $q$  is the ratio of minor to major axes and  $q_0$  is the minimum disk thickness. We set  $q_0 = 0.2$  for all galaxies. This value is a compromise, as some galaxies (e.g., Sc type) will have intrinsic  $q_0$  closer to  $\sim 0.13$  (e.g., see **REFERENCE**), while highly bulged galaxies will have larger  $q_0$ . However, as morphologies are only available for a subset of galaxies, a generic inclination correction fit our needs for homogeneity. The result is that very thin galaxies will be slightly biased towards higher inclination and vice-versa with thicker galaxies.

#### 3.36. *incErr*

Inclination error derived from the error in major and minor axes fits (see 3.25). Measurement errors for diameters, axis-ratios, and position angles are inconsistently reported in NED, so this value only captures the additional error introduced by converting non-2MASS diameters. For consistency, we set 2MASS diameter errors uniformly at 5%.

#### 3.37. *PA*

Position angle in units of degrees.

When multiple PA measurements are available for a given target, we choose the highest ranking measurement as outlined in **ref MajDiam\_ang**.

#### 3.38. *diam.key*

The observed passband of the diameter measurements. The published diameters are converted to an equivalent 2MASS  $K_s$  “total” value following the fits given in 1.

#### 3.39. *ratio.key*

The observed passband of the diameter ratio measurement. This is used to calculate the minor axis diameters and inclinations.

#### 3.40. *pa.key*

The observed passband of the position angle measurement.

#### 3.41. *RC3\_type*

Galaxy morphology as published in the Third Reference Catalog of Bright Galaxies (RC3; see de Vaucouleurs G. et al. 1994 for full description). Galaxies not included in RC3 are marked ‘x’.

#### 3.42. *RC3\_d25*

The RC3 apparent major isophotal diameter measured at the 25th magnitude surface-brightness level, in units of B-mag per arcsecond.

#### 3.43. *RC3\_r25*

The RC3 ratio of the major to minor axis diameter (converted from decimal logarithm to a straight ratio in order to match the units of *ratio.key*).

#### 3.44. *RC3\_pa*

The RC3 position angle in units of degrees.

3.45. *group\_num*

Group designation taken from the Tully (2015) group catalog.

3.46. *group\_mem*

Number of members in this galaxy group from the 2MASS 11.75 catalog (Huchra et al. 2012), taken from the Tully (2015) group catalog.

3.47. *group\_dist*

Distance to the galaxy group, taken from the Tully (2015) group catalog.

3.48. *MType*

Morphological type as homogenized by NED. We have removed extraneous space characters, and then replaced the individual spaces with underscore characters.

3.49. *flag*

A flag to help identify suspected issues with a galaxy. For most objects *flag* = 0. If, however, we suspect an object to be a star we set *flag* = 1. Our criteria for this is as follows: 1) if an object has  $V_{hel} < 500 \text{ km s}^{-1}$ , no diameter measurement, and no *MType* available, 2) if *MType* is found to match any of our exclude morphologies. Our full exclude list is the following: ['M-star', 'M\_star', 'Opt.var.', 'K4-K5;Candidate\_WD', 'F6-F8;Candidate\_WD', 'A', 'Candidate\_AGN', 'M1', 'star??', 'O', 'K\_Star', 'PN?', 'K1', 'M0', 'M0V', 'A0', 'DA-star', 'High-vel.cloud', 'O', 'Carbon', 'Point\_Src\_[SDSS]', 'Possible\_star', 'Planetary\_nebula', 'M3-M4', 'F2', 'A-star', 'PN:', 'Cand\_.glob\_.cluster', 'Candidate\_PN', 'F', '0.9', '0.92', '14', '14.247', '14.632', '14.728', '14.818', '14.998', '15.159', '15.171', '15.242', '15.341', '15.458', '15.79', '15.819', '16', '16.281', '16.309', '16.348', '16.394', '16.556', '16.736', '16.764', '16.783', '16.981', '17.012', '17.039', '17.441', '17.597', '2E', '2MASS\_Extended\_Ver.2', '2\_S0\_galaxies', '2\_S0\_pec\_galaxies', '2\_SB0?\_pec\_galaxies', '2\_Spec?', '2\_compacts', '2\_or\_3?\_spirals', '2\_spirals', '2\_symm.sp.arms', '3\_S0\_galaxies', ':', 'A', 'A-star', 'A0', 'A3\_HII', 'AGN', 'AGN+SF', 'AGN1', 'AGN2', 'AGN:', 'AGN?', 'ALG', 'Amorphous', 'B', 'B...', 'D', 'DA', 'DA+M', 'DA+M:', 'DA+M:;Cand.\_QSO', 'DA-star', 'DA', 'DA+M', 'DA+M:', 'DA+M:;Cand.\_QSO', 'DA-star', 'DA:', 'DANS', 'DANS?', 'DANS?\_Sbrst', 'DANS.WR?', 'DA\_auto', 'DBA', 'DC:', 'DGTO', 'DISRPTD', 'DISTRBD', 'DQ:', 'DQ;Cand.\_QSO', 'DSa', 'K1', 'K4-K5;Candidate\_WD', 'K\_Star', 'M', 'M-star', 'M0', 'M0V', 'M1', 'M3-M4', 'M\_Star', 'M\_star', 'Planetary\_or\_galaxy', 'Planetary?', 'Planetary\_nebula', 'Possible.\*Cl', 'Possible\_star', 'bright\_near\*', 'star:', 'star?', 'star??', 'stellar', 'stellar-like', 'stellar:']

Secondly, we set *flag* = 2 if the velocity implied by  $RID_{median}$  (i.e.,  $RID_{median} * H_0$ ) differs from  $V_{hel}$  by more than  $1500 \text{ km s}^{-1}$ . If *flag* = 2, it may be wise to use *distvcorr* instead of *bestDist*. There is no overlap between *flag* types, so no possible stars (*flag*=1) objects have a redshift independent distance available.

3.50. *distIndicator*

A key indicating which method was used to measure the redshift-independent distance for this galaxy. Table

2 shows the keys and their corresponding full names as compiled in the NED-D distance catalog. This key corresponds *only* to the  $RID_{median}$  value.

Key	Distance Indicator	Key	Distance Indicator
AGB	AGB	MagEn	Magnetic energy
AGNtl	AGN time lag	Mag	Magnitude
Bstar	B Stars	Maser	Maser
BCG	BCG	MassM	Mass Model
BH	Black Hole	Miras	Miras
BLLum	BL Lac Luminosity	Novae	Novae
BSG	Blue Supergiant	OBstr	OB Stars
Brstr	Brightest Stars	OrMec	Orbital Mech.
Cstar	Carbon Stars	PAGB	PAGB Stars
Ceph	Cepheids	PNLF	PNLF
CMD	CMD	propM	Proper Motion
dCO	CO ring diameter	QS	Quasar spectrum
Dsigm	D-Sigma	Radio	Radio Brightness
Scuti	Delta Scuti	RClum	Red Clump
Diam	Diameter	DRing	Ring Diameter
dwEll	Dwarf Ellipticals	RRLyr	RR Lyrae
Dwarf	Dwarf Galaxy Diameter	RSV	RSV Stars
EclBi	Eclipsing Binary	RV	RV Stars
FJ	Faber-Jackson	SDorS	S Doradus Stars
FGLR	FGLR	SBF	SBF
GLens	G Lens	SGRB	SGRB
GCFP	GC FP	SNia	SNia
GCKJK	GC K vs. (J-K)	SNIIo	SNII optical
GCrad	GC radius	SNIIr	SNII radio
GCLF	GCLF	SNias	SNia SDSS
GCSBF	GC SBF	Stat	Statistical
gamma	GeV TeV ratio	Sosie	Sosies
GSGD	Grav. Stability Gas. Disk	subDw	Subdwarf fitting
GRB	GRB	SXPS	SX Phe Stars
Hlod	H I + optical distribution	SZ	SZ effect
HILF	HII LF	Terti	Tertiary
dHII	HII region diameter	TRGB	TRGB
HB	Horizontal Branch	TFest	Tully est
IRAS	IRAS	TF	Tully-Fisher
Jet	Jet Proper Motion	CepII	Type II Cepheids
LHbs	L(H $\beta$ )- $\sigma$	WD	White Dwarfs
LSB	LSB galaxies	WR	Wolf-Rayet
Mstar	M Stars		

Table 2

Distance indicators and associated keys. Full descriptions can be found here <https://ned.ipac.caltech.edu/Library/Distances/distintro.html>

3.51. *lumClass*

Luminosity class as assigned by NED. Roman numerals between I, II, III, IV, and V designate galaxies in order of decreasing luminosity in an analogous fashion to the standard stellar luminosity classes.

3.52. *E(B-V)*

Galactic mean dust extinction in the direction of each galaxy from Schlafly & Finkbeiner (2011). **MORE?**

3.53. *Bmag*

The median B-band magnitude.

3.53.1. *Photometry*



For each galaxy we retrieved all B-band and SDSS  $g$ ,  $r$ , and  $z$  measurements. Direct  $B$  band measurements are available for  $\sim 30\%$  of galaxies, and most of the rest have SDSS magnitudes, which we converted to  $B$ -band via  $B = g + 0.39(g - r) + 0.21$  (Jester et al. 2005). Per SDSS DR12 guidelines, we preferentially selected SDSS *petrosian* magnitudes when available, followed by *model* and *cmodel* values if *petrosian* was not available. We then selected the min, max and median  $B$ -band values when more than one was available for inclusion in the final data product. SDSS-converted  $B$ -band values are included as a separate estimate.

We then computed each galaxy's luminosity in units of  $L_*$  for each of the min, median, max and SDSS  $B$ -band values as follows:

$$\frac{L}{L_*} = 10^{-0.4(M_B - M_{B_*})}, \quad (4)$$

where  $M_B$  is the galaxy absolute magnitude, calculated using the  $d_{best}$  distance estimate as described above. We adopted the CfA galaxy luminosity function by Marzke et al. (1994), which sets  $B_* = -19.57$ .

### 3.54. *Bmag\_key*

The survey that contributed the value of *Bmag*.

### 3.55. *Bmag\_max*

The brightest B-band magnitude available in NED for this object. See ?? for details.

### 3.56. *Bmag\_max\_key*

The survey that contributed the value of *Bmag\_max*.

### 3.57. *Bmag\_min*

The dimmest B-band magnitude available in NED for this object. See ?? for details.

### 3.58. *Bmag\_min\_key*

The survey that contributed the value of *Bmag\_min*.

### 3.59. *Bmag\_sdss*

SDSS  $g$  and  $r$ -band measurements converted to  $B$ -band via  $B = g + 0.39(g - r) + 0.21$  (Jester et al. 2005). See ?? for details.

### 3.60. *gmag\_sdss*

The SDSS  $g$ -band magnitude used in the *Bmag\_sdss* calculation.

### 3.61. *rmag\_sdss*

The SDSS  $r$ -band magnitude used in the *Bmag\_sdss* calculation.

### 3.62. *zmag\_sdss*

SDSS  $z$ -band magnitude used in the *Bmag\_sdss* calculation.

### 3.63. *Lstar\_med*

The  $L/L_*$  ratio calculated using *Bmag*, *distBest*, and  $E(B - V)$  following Eq. 4.

### 3.64. *eLstar\_med*

*Lstar\_med* error calculated with *eBmag* and *e.distBest*. Errors in  $E(B - V)$  are relatively negligible and thus were not used.

### 3.65. *Lstar\_max*

The  $L/L_*$  ratio calculated using *B\_max*, *distBest* + *dist\_err*, and  $E(B - V)$  following Eq. 4.

### 3.66. *eLstar\_max*

*Lstar\_med* error calculated with *eBmag\_max* and *e.distBest*. Errors in  $E(B - V)$  are relatively negligible and thus were not used.

### 3.67. *Lstar\_min*

The  $L/L_*$  ratio calculated using *B\_min*, *distBest* - *dist\_err*, and  $E(B - V)$  following Eq. 4.

### 3.68. *eLstar\_min*

The  $L/L_*$  ratio calculated using *eBmag\_min*, *distBest* - *dist\_err*, and  $E(B - V)$  following Eq. 4.

### 3.69. *Lstar\_sdss*

The  $L/L_*$  ratio calculated using *B\_min*, *dist\_best* - *dist\_err*, and  $E(B - V)$  following Eq. 4.

### 3.70. *eLstar\_sdss*

The  $L/L_*$  ratio calculated using *B\_min*, *dist\_best* - *dist\_err*, and  $E(B - V)$  following Eq. 4.

### 3.71. *altNames*

The NED list of alternative object names for this galaxy with spaces removed. In the main catalog we have included only NGC, IC, UGC, SDSS, and 2MASS names in this column. The associated alternative names table contains the full list. Note that our preferred name, *Name*, and *NEDname* will only appear in the *altNames* list if they match these same criteria.

## 4. SUMMARY

Summary...

This research has made use of the NASA/IPAC Extragalactic Database (NED) which is operated by the Jet Propulsion Laboratory, California Institute of Technology, under contract with the National Aeronautics and Space Administration. Based on observations with the NASA/ESA *Hubble Space Telescope*, obtained at the Space Telescope Institute, which is operated by AURA, Inc., under NASA contract NAS 5-26555.

## REFERENCES

- Schlafly, E. F., & Finkbeiner, D. P. 2011, ApJ, 737, 103  
 Stocke, J. T., Keeney, B. A., Danforth, C. W., et al. 2013, ApJ, 763, 148  
 Tully, R. B. 2015, AJ, 149, 171  
 Tully, R. B., Rizzi, L., Shaya, E. J., et al. 2009, AJ, 138, 323